IEEE Access
Multidisciplinary | Rapid Review | Open Access Journal

SPECIAL SECTION ON DATA-DRIVEN MONITORING, FAULT DIAGNOSIS AND CONTROL OF CYBER-PHYSICAL SYSTEMS

Received October 28, 2017, accepted November 28, 2017, date of publication December 4, 2017,
date of current version February 14, 2018.

Digital Object Identifier 10.1109/ACCESS.2017.2779175

Data-Based Predictive Control for Wastewater Treatment Process

HONG-GUI HAN, (Senior Member, IEEE), LU ZHANG, AND JUN-FEI QIAO, (Member, IEEE)
Beijing Key Laboratory of Computational Intelligence and Intelligent System, Faculty of Information Technology, Beijing University of Technology, Beijing 100124, China

Corresponding author: Hong-Gui Han (rechardhan@sina.com)

This work was supported in part by the National Science Foundation of China under Grant 61622301 and Grant 61533002, in part by the Beijing Natural Science Foundation under Grant 4172005, and in part by the Major National Science and Technology Project under Grant 2017ZX07104.

ABSTRACT Wastewater treatment process (WWTP) has long been a challenging industrial issue due to its built-in uncertainties and discontinuous measurement of system states. To solve this problem, in this paper, a data-based predictive control (DPC) strategy, based on the available sensing measurements, is proposed to control the dissolved oxygen (DO) concentration in WWTP. First, a self-organizing fuzzy neural network, which can adjust both the structure and parameters simultaneously, is developed to identify the real-time states of WWTP. Second, an improved nonlinear predictive control method is designed to reduce the online computation complexity by transforming the constrained conditions into an unconstrained nonlinear programming problem. Then, an adaptive second-order Levenberg-Marquardt algorithm is developed to derive the control law of DPC. Third, the theoretical analysis on the stability is also given to confirm the prerequisite of any successful application of DPC. Finally, the proposed DPC strategy is applied to the Benchmark Simulation Model No. 1. Experimental results demonstrate that the control performance of the proposed DPC is better than some existing methods.

INDEX TERMS Wastewater treatment process, data-based predictive control strategy, self-organizing fuzzy neural network, adaptive second-order Levenberg-Marquardt algorithm.

I. INTRODUCTION

Wastewater treatment is critical for modern urban societies and provides essential protections for both the aquatic environment and human health [1], [2]. A combination of physical, chemical and biological processes in wastewater treatment process (WWTP) has been used to reduce or eliminate suspended solids, organic matter, nitrogen, and phosphate [3], [4]. For this reason, WWTP is a complex system due to its nonlinear dynamics, large uncertainty, multiple time scales in the internal process reactions and multivariable structure [5], [6]. Hence, it is difficult to design an applicable controller for WWTP to meet the more and more stringent discharge and emission limits [7].

Recent developments in control methods and particularly in the model predictive control (MPC), handling problems with uncertainty, estimation, and trajectory tracking in nonlinear systems, have triggered new research and applications in this field [8]–[10]. From a practical-theoretic viewpoint, being a model-based control method, MPC is a useful technique for the control of constrained nonlinear systems [11], [12]. However, there is still a gap between theoretical MPC analysis and their practical implementation for WWTP [13], [14]. On one hand, the models of WWTP are difficult to be described, thus, the predictive control technique must be extended to incorporate the nonlinear models of WWTP. That is, the identification of WWTP is an important and necessary part of MPC. On the other hand, the computation complexity is another problem for the online optimal control of WWTP. An important aspect for a practical implementation of MPC is to use an efficient algorithm for solving the underlying optimal control problem.

To identify nonlinear and uncertain process of WWTP, many modeling methods have been derived, from simplified mechanism models to data-driven based methods [15], [16]. For example, Stare *et al*. developed an ammonia model based on nitrification reaction rate for MPC in a WWTP [15].

The results demonstrated that the proposed nonlinear ammonia model performed well compared with the linear model. In [16], a nonlinear mathematical model based on mass balances was used to model the ammonia for MPC in an activated sludge plant. However, the proposed MPC strategies are still not be suitable for different conditions. To improve the model accuracy of MPC for WWTP, the data-driven modeling methods have attracted a great deal of attention [17], [18]. Krueger *et al.* [17] proposed a data-driven scheme based on key performance indicator (KPI) for prediction and control. The efficient prediction results of the effluent flow rate were achieved. Shao *et al.* [18] presented local partial least squares (LPLS) models of selective ensemble to predict the effluent quality by the predictive control strategy. The process states were partitioned into local model regions to deal with the process nonlinearity and improve the prediction accuracy. To study the coagulation process of WWTP, a neural network based MPC was developed in [19]. In this proposed strategy, a multi-layer back-propagation neural network was introduced to model the nonlinear relationships between the removal rates of pollutants and the chemical dosages, with satisfied model accuracy. Moreover, in order to strengthen the adaptive ability, logical capacity and reasoning ability for identifying the states of WWTP, fuzzy neural networks (FNNs), owning the advantages of both neural networks and fuzzy systems, have been widely used in MPC strategies [20]–[22]. For example, a MPC strategy, based on FNN model, was proposed for a real WWTP in [21]. The results showed that this T-S fuzzy model could identify the effluent concentration adaptively. Yang *et al.*[22] investigated a FNN-based predictive controller for activated sludge wastewater treatment processes. The FNN model was derived to identify the processes in MPC to achieve satisfactory control performance. Further, some other FNN-based MPC strategies were also discussed in [23] and [24]. These MPC strategies could achieve superior identification effects and desired model accuracy to improve the control performance. However, one of the main drawbacks of these strategies is to determine the structure of FNN as fixed. As a result, most of these MPC strategies cannot handle the model structure problem under the disturbances and uncertainties of WWTP [25], [26].

Computation complexity is another challenging technical issue of MPC strategy for WWTP, it is urgent to design an efficient approach for reducing the computation complexity in the online optimal control process [27]. Recently, various approaches have been developed, e.g. in [28]–[33]. In [28], a nonlinear MPC, based on the piecewise-linearized hybrid approximation, was utilized to calculate the online control sequences. The simulation results demonstrated the efficiency of the proposed method. Muller *et al*. developed a novel switched MPC method for nonlinear wastewater systems, in which the different cost functions were switched to enhance the computational performance [29]. Moreover, an interior point nonlinear solver, according to the process economics, was introduced for MPC in [30]. The case study indicated the computational performance. Mulas *et al.* [31] developed predictive control strategy, using a simple dynamic matrix control algorithm, for controlling the nitrogen concentration in a full-scale WWTP. The dynamic matrix control algorithm could improve the computational performance and the tracking accuracy. And some other methods for reducing the computation complexity of MPC could be found in [32] and [33]. However, for these above methods, since the dynamics and the random disturbances of WWTP are hard to be obtained, it is still a challenge to design an appropriate online optimal method with suitable constraints [34].

Based on the above discussion, in this paper, a data-based predictive control (DPC) strategy is developed to realize the optimal control of WWTP. This proposed DPC strategy has its advantages to improve the model accuracy and reduce the computation complexity. The main contributions of this paper are:

1) A data-driven identifier, based on self-organizing fuzzy neural network (SOFNN), is introduced for predicting the real-time operational states of WWTP. Unlike some existing FNNs for MPC strategies [21]–[24], this proposed SOFNN identifier can adjust both the parameters and the structure to improve the predicting accuracy.
2) With the purpose of solving the optimization problem without constraints for WWTP, a DPC strategy, transforming the constrained conditions into an unconstrained nonlinear programming problem, is designed for controlling the dissolved oxygen (DO) concentration. Meanwhile, an adaptive second-order Levenberg-Marquardt algorithm is developed to derive the control law of this DPC strategy to reduce the online computation complexity.
3) As the stability is important to the applications of DPC scheme, the proposed control strategy is designed with these in mind. The stability analysis is demonstrated theoretically in details.

The remainder of this paper is organized as follows. Section II describes the overall DPC scheme, the details of parameters and rule-layer neurons adjustment process for SOFNN identifier and online calculation of the optimal control strategy. In Section III, the stability of the proposed DPC is discussed. Then, in Section IV, the simulation results are presented to demonstrate the effectiveness of DPC and the final conclusions are given in Section V.

II. DATA-BASED PREDICTIVE CONTROL (DPC) STRATEGY

A. DPC SCHEME

To realize the optimal control for WWTP, the proposed DPC scheme used in this work is presented as shown in Fig. 1. This DPC scheme mainly consists of two parts: SOFNN identifier and the online optimal control. SOFNN identifier is used to deal with the real-time state prediction under dynamical stations. Meanwhile, the online optimal control is applied to acquire the control actions for improving the control performance.

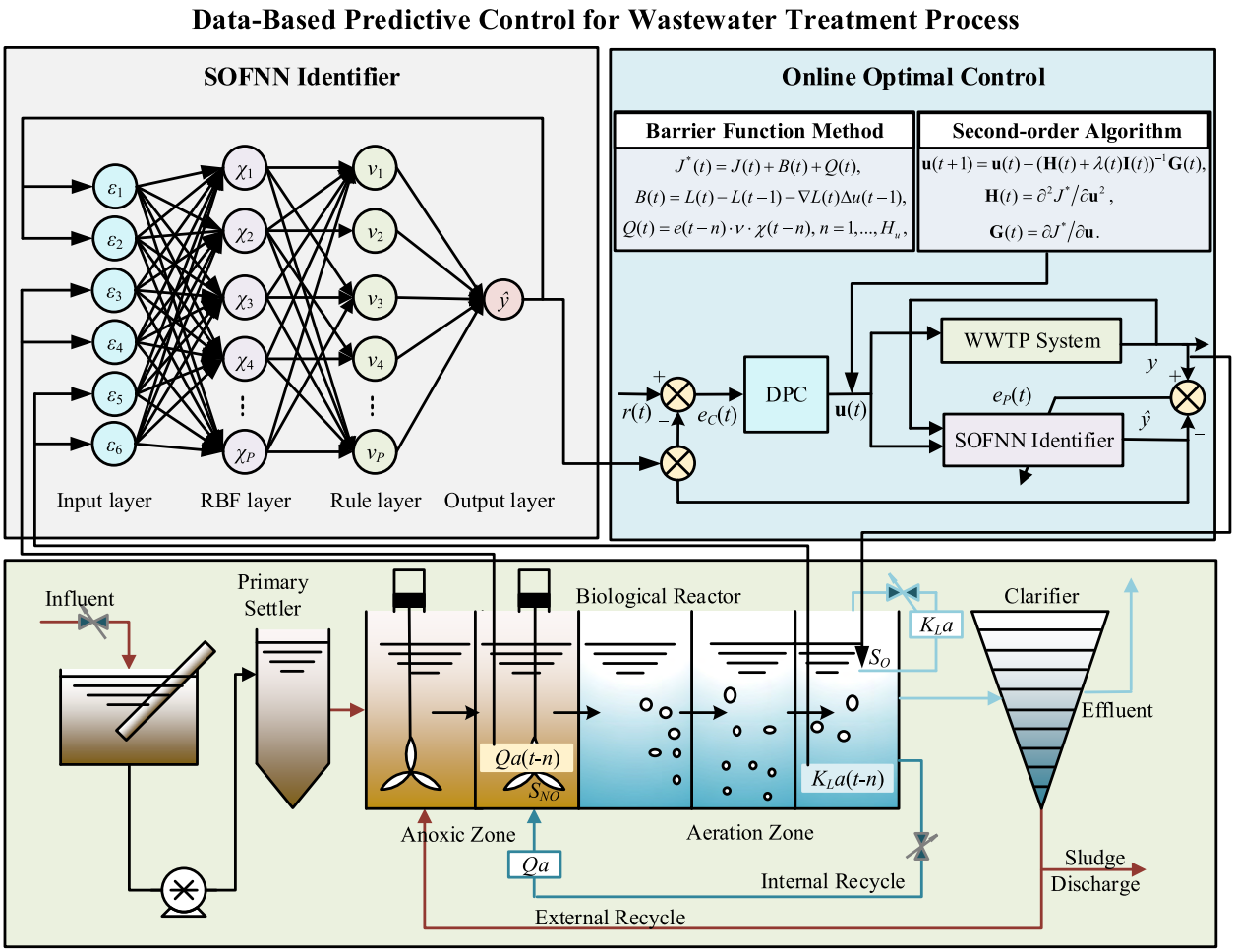

FIGURE 1. DPC scheme.

In the proposed DPC scheme, SOFNN identifier is used to predict DO concentration by means of the selection of related input variables and the adjustment of model parameters and structure. The historical data, collected from the available sensing measurements, are used to update the identifier and improve the predicting performance. The online optimal control method, transforming the constrained conditions into an unconstrained nonlinear programming problem, is then applied to control DO concentration.

B. SOFNN IDENTIFIER

To predict DO concentration online, a SOFNN is developed to approximate the multi-input-single-output (MISO) relationship between DO concentration and its influencing variables. In WWTP, DO concentration is mainly manipulated by oxygen transfer coefficient in the fifth unit (K_La_5) and the internal recycle (Q_a) simultaneously. During the reaction process, six related model inputs $y(t-1), y(t-2), K_La_5(t-5), K_La_5(t-6), Q_a(t-5), Q_a(t-6)$ are used for SOFNN identifier, $y(t-1)$ is the system output at time $t-1$, $y(t-2)$ is the system output at time $t-2$, $K_La_5(t-5)$ is the oxygen transfer coefficient at time $t-5$, $K_La_5(t-6)$ is the oxygen transfer coefficient at time $t-6$, $Q_a(t-5)$ is the internal recycle at time $t-5$, and $Q_a(t-6)$ is the internal recycle at time $t-6$. In this SOFNN, four layers - the input layer, the radial basis function (RBF) layer, the rule layer and the output layer, are included, and the output is described as:

$$\hat{y}(t) = f(\boldsymbol{\varepsilon}(t), \boldsymbol{\chi}(t), \mathbf{v}(t)) = \sum_{l=1}^{P} w_l(t) e^{-\sum_{i=1}^{6} \frac{(\varepsilon_i(t)-c_{il}(t))^2}{2\sigma_{il}^2}(t)} \Big/ \sum_{j=1}^{P} e^{-\sum_{i=1}^{6} \frac{(\varepsilon_i(t)-c_{ij}(t))^2}{2\sigma_{ij}^2}(t)}, \tag{1}$$

where $\hat{y}(t)$ is the predicted output of SOFNN, $f(\cdot)$ is the mapping function, $\boldsymbol{\varepsilon}(t)$ are the model inputs, and $\boldsymbol{\varepsilon}(t) = [y(t-1), y(t-2), K_La_5(t-5), K_La_5(t-6), Q_a(t-5), Q_a(t-6)]$, $\boldsymbol{\chi}(t) = [\chi_1(t), \chi_2(t), \ldots, \chi_P(t)]^{\mathrm{T}}$ are the outputs of RBF layer, $\mathbf{v}(t) = [v_1(t), v_2(t), \ldots, v_P(t)]^{\mathrm{T}}$ are the outputs of rule layer, P is the number of neurons in RBF layer and the rule layer, $\mathbf{c}_j(t) = [c_{1j}(t), c_{2j}(t), \ldots, c_{6j}(t)]$ and $\boldsymbol{\sigma}_j(t) = [\sigma_{1j}(t), \sigma_{2j}(t), \ldots, \sigma_{6j}(t)]$ are the vectors of centers and widths of the jth neuron in RBF layer, respectively,

$\mathbf{w}(t) = [w_1(t), w_2(t), \ldots, w_P(t)]$ are the weights between the output layer and the rule layer.

In SOFNN model, the parameters of $\mathbf{c}(t)$, $\boldsymbol{\sigma}(t)$ and $\mathbf{w}(t)$ are updated as:

$$\begin{cases} \mathbf{c}(t+1) = \mathbf{c}(t) - \eta_1 \, \partial E(t)/\partial \mathbf{c}(t) \\ \boldsymbol{\sigma}(t+1) = \boldsymbol{\sigma}(t) - \eta_2 \, \partial E(t)/\partial \boldsymbol{\sigma}(t) \\ \mathbf{w}(t+1) = \mathbf{w}(t) - \eta_3 \, \partial E(t)/\partial \mathbf{w}(t), \end{cases} \tag{2}$$

where η_1, η_2 and η_3 are the positive learning rates, $\mathbf{c}(t) = [\mathbf{c}_1(t), \mathbf{c}_2(t), \ldots, \mathbf{c}_P(t)]$, $\sigma(t) = [\sigma_1(t), \sigma_2(t), \ldots, \sigma_P(t)]$, $E(t)$ is the sum of squared error between real output and predicting value

$$E(t) = \frac{1}{2}e^2(t) = \frac{1}{2}(y(t) - \hat{y}(t))^2. \tag{3}$$

Moreover, the structure of SOFNN is adjusted by the relative importance index (RII) and $E(t)$. RII is used to compute the proportion of the output values based on the input parameters [35], [36]. The influence index, evaluated by the values of neurons in the rule layer that generated to the output layer, is expressed as $\mathbf{R}(t)$, where $\mathbf{R}(t) = [R_1(t), R_2(t), \ldots, R_P(t)]$.

In the adjustment process of neurons in the rule layer, if the condition meets

$$E(t) > E(t-1), \tag{4}$$

the neuron with largest relative importance index $R_m(t)$ will be split, where $R_m(t) = \max \mathbf{R}(t)$, and a new neuron will be added in the rule layer to improve the model performance. Meanwhile, the parameters of the new inserted neuron are adjusted as [37].

If the current conditions satisfy

$$\begin{cases} E(t) < E(t-1) \\ R_h(t) \le R_r, \end{cases} \tag{5}$$

where $R_r \in (0, R_{r0})$, R_{r0} is the threshold, and $R_h(t) = \min \mathbf{R}(t)$, then the hth neuron in the rule layer will be deleted and the parameters of remained neurons will be updated as [37]. The procedures for adjusting SOFNN are summarized in Table 1.

Remark 1: A MISO SOFNN is developed in the proposed DPC strategy to predict DO concentration for WWTP. During the predicting process, both the model parameters $\mathbf{w}$, $\mathbf{c}$, $\boldsymbol{\sigma}$ and the model structure can be updated to improve the modeling performance.

C. ONLINE OPTIMAL CONTROL

In this proposed DPC strategy, the cost function $J(t)$ is designed as:

$$J(t) = \sum_{i=1}^{H_P}(r(t) - \hat{y}(t+1))^2 + \rho \sum_{j=1}^{H_u} \Delta\mathbf{u}(t+j-1)^{\mathrm{T}} \times \Delta\mathbf{u}(t+j-1) + B_{u1}(t) + B_{u2}(t), \tag{6}$$

where H_p is the prediction horizon and H_u is the control horizon ($H_u < H_p$), $r(t)$ is the reference of DO concentration,

TABLE 1. Details of SOFNN updating process.

For input $\boldsymbol{\varepsilon}(t)$
% Update the model parameters
  for all weights, centers and radii in RBF layer
    update $\mathbf{w}(t)$, $\mathbf{c}(t)$ and $\boldsymbol{\sigma}(t)$; %Eq.(2)
  end
% Adjust the neurons in rule layer
  for all hidden neurons in rule layer
    calculate $R(t)$ and $E(t)$;
  end
  if $E(t)$> $E(t$-1) %Eq.(4)
    add a new neuron by splitting the neuron with the largest RII and update the parameters;
  end
  if $E(t)$> $E(t$-1) and $R_{\mathrm{h}}(t)$<R_r %Eq.(5)
    delete the hth neuron and update the parameters of nearest neuron;
  end
end

$\hat{y}(t)$ is the predicted output of DO concentration, ρ is the penalty parameter, $\Delta\mathbf{u}(t)$ are the control variations, $\Delta\mathbf{u}(t) = \mathbf{u}(t) - \mathbf{u}(t-1)$, $\mathbf{u}(t) = [u_1(t), u_2(t)]^{\mathrm{T}} = [K_L a_5(t), Q_a(t)]^{\mathrm{T}}$, $0\ \mathrm{d}^{-1} < u_1(t) < 240\ \mathrm{d}^{-1}$, $0\ \mathrm{m}^3/\mathrm{d}^{-1} < u_2(t) < 95530\ \mathrm{m}^3/\mathrm{d}^{-1}$, $B_{u1}(t)$ and $B_{u2}(t)$ are the barrier functions

$$\begin{aligned} B_{u1}(t) &= -\mu_1(t)\ln(240 - u_1(t)) - \mu_2(t)\ln u_1(t) \\ B_{u2}(t) &= -\xi_1(t)\ln(95530 - u_2(t)) - \xi_2(t)\ln u_2(t), \end{aligned} \tag{7}$$

where μ_1, μ_2, ξ_1, ξ_2 are the weighting parameters used to determine the influence of $B_{u1}(t)$ and $B_{u2}(t)$

$$\begin{cases} \mu_1(t) = ((240 - u_1(t))/(1 - \beta_1^2)u_1(t)) \cdot \nabla B_{u1}(t-1) \\ \mu_2(t) = \nabla B_{u1}(t-1), \end{cases} \tag{8}$$

$$\begin{cases} \xi_1(t) = ((95530 - u_2(t))/(1 - \beta_2^2)u_2(t)) \cdot \nabla B_{u2}(t-1) \\ \xi_2(t) = \nabla B_{u2}(t-1), \end{cases} \tag{9}$$

where $\beta_1 \in (0, 1)$, $\beta_2 \in (0, 1)$, $\nabla B_{u1}(t-1)$ and $\nabla B_{u2}(t-1)$ are the derivatives of $B_{u1}(t-1)$ and $B_{u2}(t-1)$, respectively.

At each time t, the cost function $J(t)$ is minimized to acquire the control sequences $\mathbf{u}(t)$ in DPC strategy. To guarantee the optimization performance and reduce the calculation time, an adaptive second-order L-M optimization algorithm is introduced to solve the optimization problem. Based on the online optimal control problem as described in Eq. (6), the updated rule is

$$\mathbf{u}(t+1) = \mathbf{u}(t) + \mathbf{h}(t), \tag{10}$$

where $\mathbf{u}(t)$ are the control input sequences, $\mathbf{h}(t)$ is the search direction

$$\mathbf{h}(t) = -(\mathbf{H}(t) + \lambda(t)\mathbf{I}(t))^{-1}\mathbf{G}(t), \tag{11}$$

TABLE 2. Details of the online optimal contorl scheme.

For $\mathbf{r}(t)$, suppose that $\mathbf{u}(t)$ is the optimal control sequences
% Predicting the system output
calculate the predicted outputs over prediction horizon $\hat{y}(t+1),\ldots\hat{y}(t+H_p)$ %Eq.(1)
% Solving the online optimal control problem
calculate $\mathbf{H}(t)$, %Eq.(12)
calculate $\mathbf{G}(t)$; %Eq.(13)
calculate $\lambda(t)$; %Eq.(14)
calculate $\mathbf{h}(t)$; %Eq.(11)
calculate $\mathbf{u}(t+1)$; %Eq.(10)
end

where $\mathbf{H}(t)$ is the Hessian matrix calculated at time t, $\mathbf{G}(t)$ is the gradient vector derived at time t, $\lambda(t)$ is the adaptive parameter used to assure that the matrix to be inverted is positive definite. $\mathbf{H}(t)$, $\mathbf{G}(t)$ and $\lambda(t)$ are calculated as

$$\mathbf{H}(t) = \partial^2 J(t)/\partial \mathbf{u}^2(t), \tag{12}$$
$$\mathbf{G}(t) = \partial J(t)/\partial \mathbf{u}(t), \tag{13}$$
$$\lambda(t) = \varpi(t)\lambda(t-1), \tag{14}$$
$$\varpi(t) = (\tau^{\min}(t) + \lambda(t-1))/(\tau^{\max}(t) + 1), \tag{15}$$

where $\tau^{\max}(t)$ and $\tau^{\min}(t)$ are the maximum and minimum eigenvalues of $\mathbf{H}(t)$, respectively. In the calculation process, the updated rule of the control sequences $\mathbf{u}$ is computed directly by the vector operations, therefore, the adaptive second-order L-M algorithm has the ability to reduce the storage and speed the optimal control efficiency. The online optimal control scheme can be summarized in Table 2.

Remark 2: The online optimal control is realized at each sample time based on a sequence of control input sequences $\mathbf{u}$. Taking advantage of the barrier function method and adaptive second-order L-M optimization algorithm, computation complexity is reduced in the optimal control process.

III. STABILITY ANALYSIS OF DPC STRATEGY

With respect to the stability of the nonlinear DPC system, the following assumptions and propositions are introduced.

Assumption 1: 1): The value of the penalty parameter $\rho \neq 0$. 2): The prediction error beyond the prediction horizon $e(t + H_P + 1) = 0$;

Proposition 1: 1): By taking advantage of Th. 4 in [38], it can be concluded that if $\mathbf{u}(t-1)$ satisfy Eq. (6) for $r(t-1)$, then $\mathbf{u}(t)$ satisfies Eq. (6) for $r(t)$. As $\mathbf{u}(0)$ are feasible at $t = 0$, it can be proved recursively that $\mathbf{u}(t)$ are feasible at all time $t \geq 0$. 2): As it is shown in [39], the convergence of this proposed SOFNN model can be maintained.

Theorem 1: Consider the online optimal control problem presented in Eqs. (6)-(9), and the control law designed as Eq. (10), if Assumption 1 and Proposition 1 hold, the stability of the control system can be guaranteed.

Proof: The cost function at time t is described as

$$J(t) = \sum_{i=1}^{H_P} (r(t) - \hat{y}(t+i))^2 + \rho \sum_{j=1}^{H_u} \Delta \mathbf{u}(t+j-1)^{\mathrm{T}} \times \Delta \mathbf{u}(t+j-1) + B_{u1}(t) + B_{u2}(t). \tag{16}$$

For DPC, $\mathbf{u}_1(t) = [u_1(t), u_1(t+1), \ldots, u_1(t+H_u-1)]^{\mathrm{T}}$ and $\mathbf{u}_2(t) = [u_2(t), u_2(t+1), \ldots, u_2(t+H_u-1)]^{\mathrm{T}}$ are the optimal control sequences at time t. Then, the suboptimal control sequences at time $t+1$ are set as

$$\begin{aligned}&\mathbf{u}_1^*(t+1)\\ &= [u_1(t+1), u_1(t+2), \ldots, u_1(t+H_u-1), u_1(t+H_u-1)]^{\mathrm{T}},\\ &\mathbf{u}_1^*(t+1)\\ &= [u_2(t+1), u_2(t+2), \ldots, u_2(t+H_u-1), u_2(t+H_u-1)]^{\mathrm{T}},\end{aligned} \tag{17}$$

$\mathbf{u}^*(t+1) = [\mathbf{u}_1^*(t+1), \mathbf{u}_2^*(t+1)]^{\mathrm{T}}$, then, for the suboptimal control $\mathbf{u}^*(t+1)$, the cost function is define as

$$J^*(t+1) = \sum_{i=2}^{H_P+1} e^2(t+i) + \rho \sum_{j=2}^{H_u+1} \Delta \mathbf{u}^2(t+j-1) + B_{u1}(t+1) + B_{u2}(t+1). \tag{18}$$

Based on the above analysis,

$$\begin{aligned}&J^*(t+1) - J(t)\\ &= e^2(t+H_P+1) - e^2(t+1) - \rho \Delta \mathbf{u}^2(t)\\ &\quad + B_{u1}(t+1) - B_{u1}(t) + B_{u2}(t+1) - B_{u2}(t).\end{aligned} \tag{19}$$

Taking into account $e(t + H_P + 1) = 0$ in Assumption 1, then

$$J^*(t+1) - J(t) = e^2(t+1) - \rho \Delta \mathbf{u}^2(t) + B_{u1}(t+1) - B_{u1}(t) + B_{u2}(t+1) - B_{u2}(t). \tag{20}$$

To analyze the difference between $B_{u1}(t+1)$ and $B_{u1}(t)$, the derivate of $B_{u1}(t)$ is shown as

$$\begin{aligned}\nabla B_{u1}(t) &= \frac{\mu}{240 - u_1(t)} - \frac{\mu_2}{u_1(t)}\\ &= \frac{(\mu_1 + \mu_2)u_1(t) - 240\mu_2}{(240 - u_1(t))u_1(t)},\end{aligned} \tag{21}$$

taking the expressions of μ_1, μ_2 into Eq. (21), we get (22), as shown at the bottom of the next page, where $\beta_1 \in (0, 1)$, $1/(1-\beta_1)^2 > 1$, and we get (23), as shown at the bottom of the next page, therefore, $\Delta B_{u1}(t) = B_{u1}(t+1) - B_{u1}(t) < 0$. In the similar way, $B_{u2}(t+1) - B_{u2}(t) < 0$. Then

$$J^*(t+1) - J(t) \leq 0. \tag{24}$$

Using these considerations, it can be concluded that, if $\mathbf{u}(t+1)$ is the optimal solution at time $t+1$, then $J(t+1) \leq J^*(t+1)$ as $\mathbf{u}^*(t+1)$ is the suboptimal one. Finally

$$\Delta J(t+1) = J(t+1) - J(t) \leq J^*(t+1) - J(t) \leq 0, \tag{25}$$

Taking advantage of the conclusions in [40], it can be observed that both $B_{u1}(t)$ and $B_{u2}(t)$ are bounded.

Therefore, the cost function $J(t)$ is monotonically decreased and bounded with respect to time and the control system is stable.

IV. EXPERIMENTS DESIGN AND RESULTS ANALYSIS

In this section, the proposed DPC strategy is researched to control DO concentration in WWTP. In order to show the evaluation and comparison with other control strategies, DPC strategy is applied to benchmark simulation model No. 1 (BSM1) to show its control performance. All the simulations are programmed with MATLAB, version 2015, and run on a PC with a clock speed of 2.6 GHz and 4 GB RAM, in a Microsoft Windows 7.0 environment.

A. WWTP SYSTEM LAYOUTS

WWTP is a nonlinear system, subject to large perturbations in influent flow rate and pollutant load, together with some constraints during the operational process. Many control strategies have been proposed to realize the close-loop control of WWTP, but their evaluation and comparison are difficult, due to the variability of the influent, the complexity of the biological and biochemical phenomena, the large range of time constants and the lack of standard evaluation criteria. To enhance the acceptance of the improved control strategy and compare the performance of the designed controller, a benchmark platform, BSM1, is introduced to evaluate the control results through two levels, one concerns the local control loops, assessed by integral of the absolute error (*IAE*), and the other provides measures for the effect on plant performance, such as aeration energy (*AE*). The system layouts of WWTP are described from three aspects, the samples, effluent bounds, and disturbances.

(1) Samples: Two-week operating data from three different weathers are derived to evaluate the control performance-dry, rain and storm.
(2) Effluent Bounds: The effluents should satisfy the discharge standards, the limits of ammonium (S_{NH}), total nitrogen (N_{tot}), suspended solid (SS), biological oxygen demand over a 5-day period (BOD_5) and chemical oxygen demand (COD) are shown as: $S_{NH} \leq 4$ mg/L, $N_{tot} \leq 18$ mg/L, $SS \leq 30$ mg/L, $BOD_5 \leq 10$ mg/L, and $COD \leq 100$ mg/L.
(3) Disturbances: To demonstrate the robustness of the proposed DPC strategy, both the influent flow rate Q_0 and the influent ammonia nitrogen NH_0 are considered as disturbances, the variations are shown in Figs. 2-3.

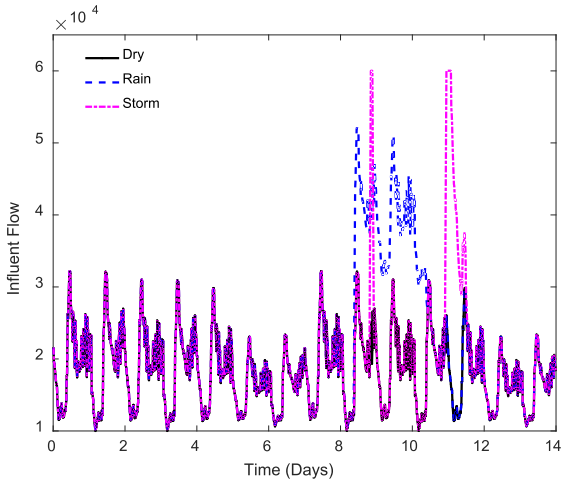

FIGURE 2. Influent flow rate Q_0.

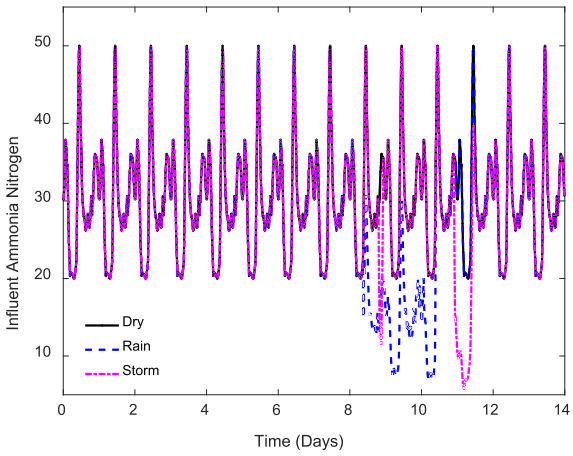

FIGURE 3. Influent ammonia nitrogen NH_0.

B. DPC STRATEGY RESULTS

Two cases with fixed optimal set-points and time-varying optimal set-points are introduced to evaluate the performance of the proposed DPC strategy.

Case 1 (Fixed Optimal Set-Points): To reflect the prediction performance of SOFNN, both the number of hidden neurons in rule layer and mean squared error (*MSE*) are

$$\nabla B_{u1}(t) = \frac{((240 - u_1(t))/((1-\beta_1)^2 u_1(t))\nabla B_{u1}(t-1) + \nabla B_{u1}(t-1))u_1(t) - 240\nabla B_{u1}(t-1)}{(240 - u_1(t))u_1(t)} \tag{22}$$

$$\begin{aligned}\nabla B_{u1}(t) &= \frac{(240 - u_1(t))/((1-\beta_1)^2 u_1(t))\nabla B_{u1}(t-1) + \nabla B_{u1}(t-1))u_1(t) - 240\nabla B_{u1}(t-1)}{(240 - u_1(t))u_1(t)} \\ &< \frac{((240 - u_1(t))/u_1(t)\nabla B_{u1}(t-1) + \nabla B_{u1}(t-1))u_1(t) - 240\nabla B_{u1}(t-1)}{(240 - u_1(t))u_1(t)} = 0,\end{aligned} \tag{23}$$

TABLE 3. The performance comparison of different methods.

Weather	Model	Hidden Neurons	*MSE* (five-step) (mg/L)
Dry	**SOFNN**	**9**	**0.0100**
	SORBF [13]	12±1*	0.0130*
	DFNN [43]	16	0.0250
	GGAP-RBF [44]	12	0.0206
	MLP [41]	15	0.0386
Rain	**SOFNN**	**12**	**0.0126**
	SORBF [13]	13±1*	0.0132*
	DFNN [43]	18	0.0341
	GGAP-RBF [44]	14	0.0903
	MLP [41]	15	0.0901
Storm	**SOFNN**	**11**	**0.0122**
	SORBF [13]	11±1*	0.0127
	DFNN [43]	17	0.0355
	GGAP-RBF [44]	12±1	0.0193
	MLP [41]	15	0.0623

applied. The calculation of *MSE* is shown as

$$MSE = \int_{t=0}^{t=14} (y(t) - \hat{y}(t))^2/14. \quad (26)$$

The model parameters are set as follows, the model input and output orders $n_y = 2$, $n_u = 2$, the delay time $t_d = 4$, the learning rate $\lambda = 0.8$, the pruning threshold $R_r 0 = 0.1$. The model inputs are $y(t-1)$, $y(t-2)$, $K_L a_5(t-5)$, $K_L a_5(t-6)$, $Q_a(t-5)$, and $Q_a(t-6)$, the prediction horizon $H_p = 5$. There are 10 initial hidden neurons in RBF layer and rule layer. And the parameters in RBF layer and rule layer are initialized randomly. The prediction results of fixed set-points in the three weathers are shown in Table 3.

To reflect the prediction performance, SOFNN model is compared with other modeling methods, self-organizing radial basis function (SORBF) [13], dynamic fuzzy neural network (DFNN) [43], generalized growing and pruning algorithm for RBF (GGAP-RBF) [44] and multi-layer perceptron (MLP) model [41]. Model parameters of SORBF, DFNN, GGAP-RBF, and MLP are similar to the original papers to guarantee the fair comparison. All results were averaged based on 20 independent runs.

Clearly, the prediction results obtained by the proposed SOFNN model are more accurate than those obtained from the other modeling methods. Performance is assessed using the number of hidden neurons in rule layer and *MSE*. From Table 3, it can be observed the proposed SOFNN model achieves with compact structure and minimal *MSE* in the three weathers. The finally hidden neurons of the SOFNN model in dry, rain and storm weathers are 9, 12 and 11 respectively. Compared with SORBF, DFNN, GGAP-RBF, and MLP, this proposed modeling method obtains with minimal hidden neurons. In addition, the prediction results acquired

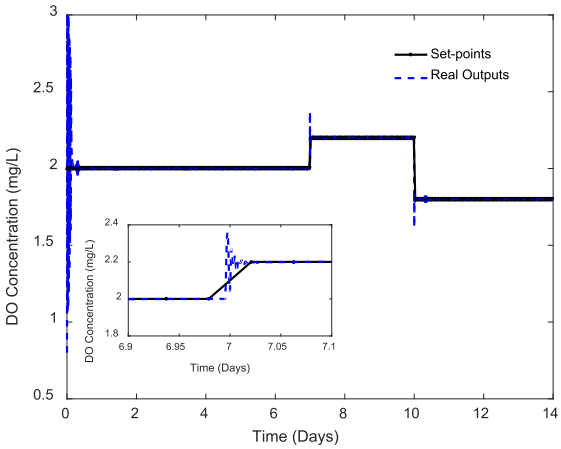

FIGURE 4. DO tracking control effects in dry weather.

by SOFNN model is more accurate than other modeling methods. *MSE* in the three weathers are 0.0100 mg/L, 0.0126 mg/L and 0.0122 mg/L respectively. The prediction results demonstrate the effectiveness of the proposed SOFNN method. The comparisons indicate that the proposed SOFNN model is more suitable for modeling nonlinear WWTP.

Taking advantage of SOFNN model, the proposed DPC strategy is carried out to realize the online optimal control. The parameters in the control process are set as follows: the penalty parameters $\rho = 10^{-2}$, the control horizon $H_u = 1$. *AE*, *IAE* and mean error (*ME*) are introduced to evaluate the control performance, the expressions are shown as:

$$AE = \frac{24}{7} \int_{t=0}^{t=14} \sum_{l=3}^{5} \left[0.0007 \times K_L a_l(t)^2 \left(\frac{V_l}{1333}\right) + 0.3267 \times K_L a_i(t) \left(\frac{V_l}{1333}\right) \right] dt, \quad (27)$$

where $(K_L a)_l$ is the overall mass transfer coefficient in the lth unit, V_l is the volume of the lth aerobic zones. In this case, a rough estimation of average electricity price in the EU (0.1 €/kWh) is taken into account, and thus, all of the weights were multiplied by 0.1.

$$IAE = \int_{t=0}^{t=14} |e_c(t)| dt, \quad (28)$$

$$ME = \int_{t=0}^{t=14} e_c(t) dt/14, \quad (29)$$

where $e_c(t)$ is the control error, $e_c(t) = y(t) - r(t)$.

Figs. 4-15 give tracking control results of the proposed DPC strategy with fixed DO concentration in three weathers during the two weeks, including the real process responses and the manipulated variables used for adjusting the control variables to realize the tracking control with the above parameter settings.

The graphs in Fig. 4 demonstrate that DPC strategy can trace the set-points of DO in dry weather. The errors in Fig. 5 show the differences between the set-points and

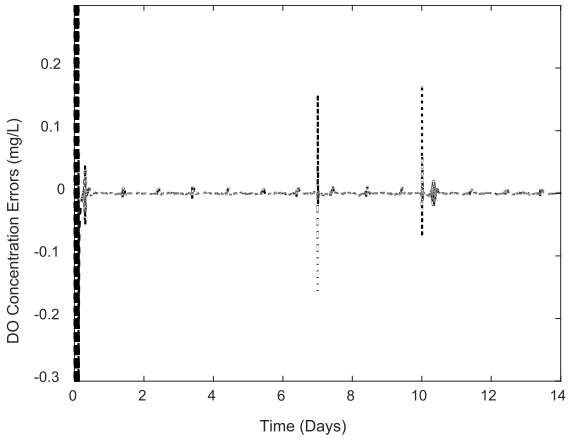

FIGURE 5. DO tracking control errors in dry weather.

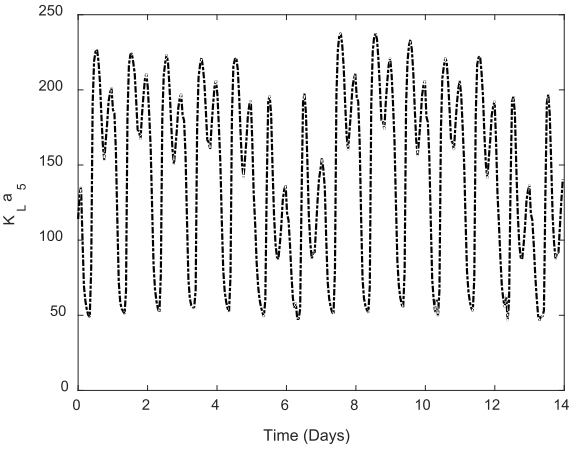

FIGURE 6. Manipulated variable $K_L a_5$ in dry weather.

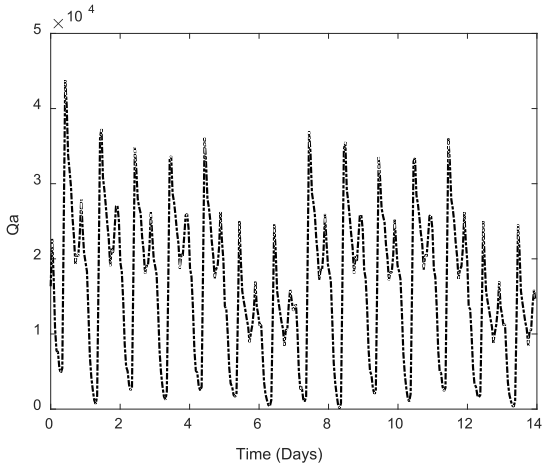

FIGURE 7. Manipulated variable Qa in dry weather.

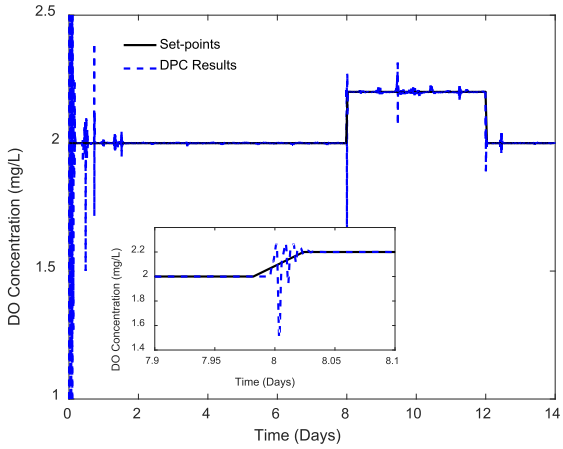

FIGURE 8. DO tracking control effects in rain weather.

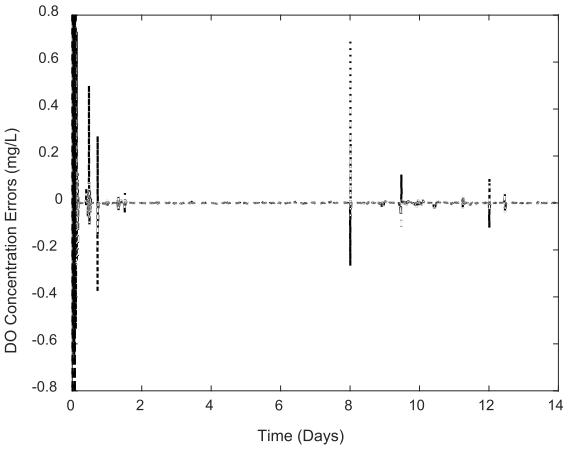

FIGURE 9. DO tracking control errors in rain weather.

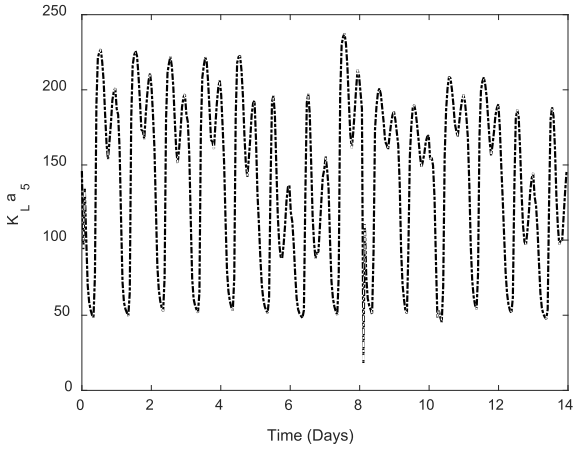

FIGURE 10. Manipulated variable $K_L a_5$ in rain weather.

the control outputs remain within the range of ±0.05 mg/L (±2.5%) except for the catastrophe points. Figs. 4-5 indicate that the proposed DPC strategy can trace DO concentration with high accuracy when the optimal set-points are fixed. The control results are smooth. In addition, the variation of two manipulated variables are presented in Figs. 6-7. Both the two manipulated variables are kept within the constrained ranges.

Tracking control results under rain weather are displayed in Figs. 8-9. As it is shown in Fig. 8, good tracking control ability is realized by DPC strategy. The errors are displayed

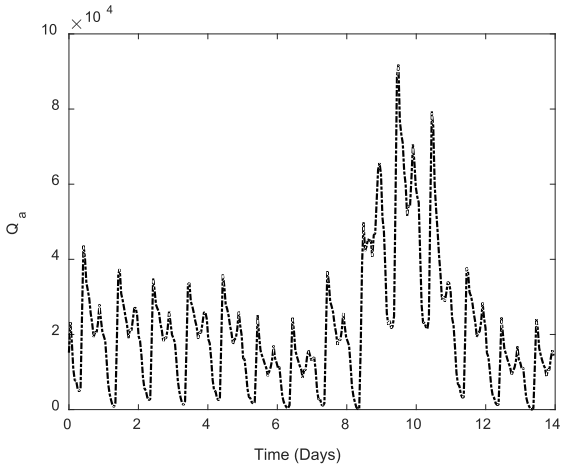

FIGURE 11. Manipulated variable Qa in rain weather.

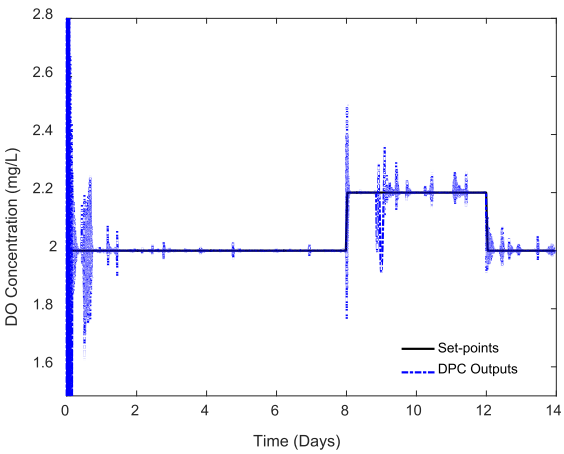

FIGURE 12. DO tracking control effects in storm weather.

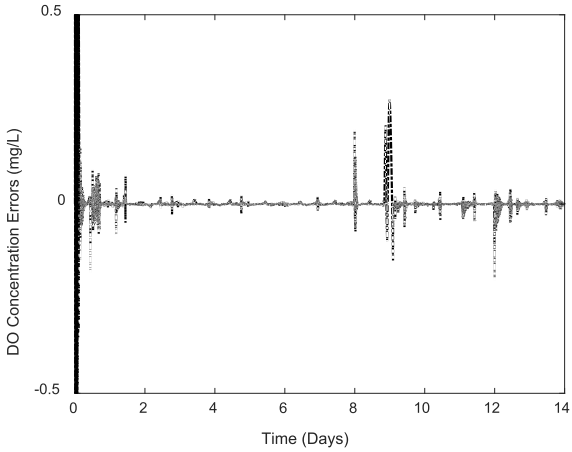

FIGURE 13. DO tracking control errors in storm weather.

in Fig. 9, and they are kept in the range of ±0.1 mg/L except for several points. Meanwhile, Figs. 10-11give the variations of $K_L a_5$ and Q_a, which are smooth.

The on-line control results under storm weather are presented in Figs. 12-15, including the real process response and

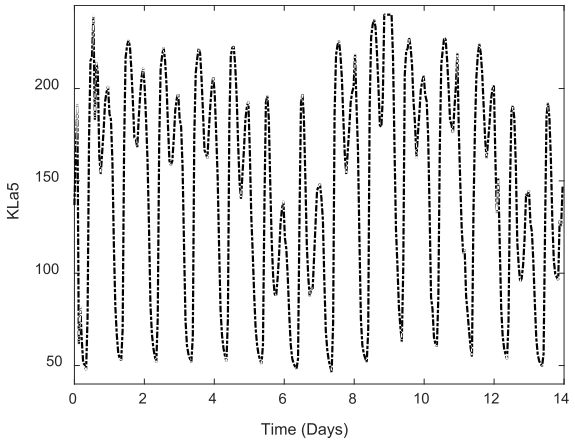

FIGURE 14. Manipulated variable $K_L a_5$ in storm weather.

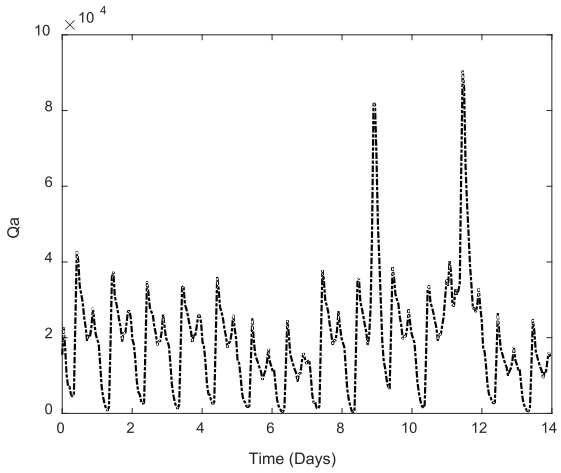

FIGURE 15. Manipulated variable Q_a in storm weather.

the variation of the manipulated variables. From Fig. 12, it is clearly observed that the real outputs follow the set-points of DO immediately. The differences between the real outputs and the set-points are described in Fig. 13. The errors stay in the range of ±0.3 mg/L. Figs. 14-15 show the variation of $K_L a_5$ and Q_a, which remain in the constrained ranges.

To evaluate the control performance, the proposed DPC strategy is compared with other existing controllers that are designed for WWTP: the proportional-integral (PI) controller [3], MPC [7], adaptive controller based on a dynamic structure neural network (ACDSNN) [42], self-organizing fuzzy controller (SOFC) [9], self-organizing recurrent radial basis function based nonlinear model predictive control (SR-RBF-NMPC) [27] and self-organizing radial basis function based MPC (SORBF-MPC) [13]. The details of the comparisons under the three weathers are shown in Table 4.

From Table 4, it is clearly seen that DPC strategy can realize the tracking control with high control accuracy when the optimal set-points are fixed. In case 1, *IAE* and *ME* of DPC strategy are 0.0094 mg/L, 0.0025 mg/L, 0.0119 mg/L, 0.0034 mg/L and 0.023 mg/L, 0.0086 mg/L in dry weather,

TABLE 4. Control performance comparison of different methods in case 1.

Weather	Controller	Rise Time (h)	Peak Time (h)	*IAE* (mg/L)	*ME* (mg/L)	*AE*(€/d)
Dry	**DPC**	**0.78**	**1.00**	**0.0094**	**0.0025**	**665**
	PI [3]	0.81	1.008	0.218*	0.112	678*
	MPC [7]	0.90	1.13	0.089*	0..078*	672
	ACDSNN [42]	1.01*	--	--	0.011*	--
	SOFC [9]	1.32	1.44	0.018*	0.020*	--
	SR-RBF-NMPC [27]	--	--	0.046*	--	667*
	SORBF-MPC [13]	--	--	0.107*	--	673
Rain	**DPC**	**0.72**	**1.08**	**0.0119**	**0.0034**	**667**
	PI [3]	0.73	1.01	0.139	0.125	698
	MPC [7]	1.13	1.22	0.150	0.097	692
	ACDSNN [42]	1.01*	--	--	0.017	--
	SOFC [9]	1.34	1.65	0.031*	0.036*	--
	SR-RBF-NMPC [27]	--	--	0.063*	--	670*
	SORBF-MPC [13]	--	--	0.119*	--	689*
Storm	**DPC**	**0.84**	**1.08**	**0.023**	**0.0086**	**680**
	PI [3]	0.84	1.01	0.153	0.109	698
	MPC [7]	1.14	1.22	0.105		687
	ACDSNN [42]	1.01*	--	--	0.012*	--
	SOFC [9]	1.34	1.50	0.025*	0.0097*	--
	SR-RBF-NMPC [27]	--	--	0.086	--	681
	SORBF-MPC [13]	--	--	0.064*	--	683

'*' denotes the result is listed in the original paper, '--' denotes none.

rain weather and storm weather respectively. In addition, the rise time and peak time in the three weathers are 0.78 h, 1.00 h, 0.72h, 1.08 h and 0.84 h, 1.08 h, which are faster than other compared control methods. The rapidity depends on not only the constraints transformation by barrier function method but also the adaptive second-order L-M algorithm for calculating the control sequences. *AE* in DPC strategy is the lowest compared with other approaches under different weathers, the average *AE* are 665 €/d, 667 €/d and 680 €/d.

Case 2 (Time-Varying Optimal Set-Points): The prediction results of SOFNN model for time-varying optimal set-points in dry weather, rain weather and storm weather are shown in Table 5. The prediction results are also compared with SORBF [13], DFNN [43], GGAP-RBF [44] and MLP [41].

From Table 5, it can be concluded that the proposed SOFNN model is appropriate for modeling the nonlinear WWTP. Both the hidden neurons and *MSE* are introduced to reflect the model performance. It is clearly observed that the proposed SOFNN method can achieve with compact model structure and minimal *MSE*. The finally structure of the SOFNN model in the three weathers are 9, 10 and 10 respectively. Compared with other modeling methods, this proposed SOFNN model obtains with the minimal hidden neurons. Meanwhile, *MSE* under the three weathers are 0.0305 mg/L, 0.0379 mg/L and 0.0422 mg/L. The prediction results indicate the effectiveness of SOFNN model.

The tracking control results of time-varying optimal set-points under the three weathers are presented in Figs. 16-27. Good tracking control ability by DPC strategy are observed from Fig. 16 in spite of the frequent changes of the set-points.

TABLE 5. The performance compatison of different methods.

Weather	Model	Hidden Neurons	*MSE*(five-step) (mg/L)
Dry	**SOFNN**	**9**	**0.0305**
	SORBF [13]	13±1*	0.0691*
	DFNN [43]	18	0.0720
	GGAP-RBF [44]	12	0.0811
	MLP [41]	15	0.0916
Rain	**SOFNN**	**10**	**0.0379**
	SORBF [13]	13±1	0.0692*
	DFNN [43]	13	0.0835
	GGAP-RBF [44]	14±1	0.0903
	MLP [41]	15	0.0981
Storm	**SOFNN**	**10**	**0.0422**
	SORBF [13]	11±1	0.0701
	DFNN [43]	18	0.0846
	GGAP-RBF [44]	12	0.0936
	MLP [41]	15	0.0992

The control errors are displayed in Fig. 17 and remain within the range of ±0.01 mg/L except for the catastrophe points. Figs. 16-17 indicate that DPC strategy can track DO concentration accurately. The variation of two manipulated variables are given in Figs. 18-19.

Tacking control results in rain weather are presented in Figs. 20-23. Taking advantage of the proposed DPC strategy, it is clearly seen that satisfied tracking control results are

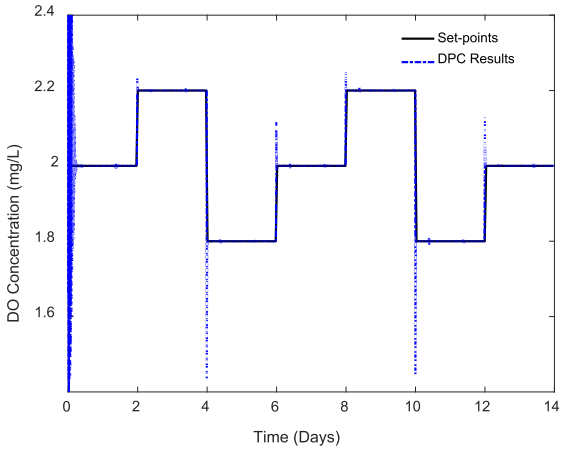

FIGURE 16. DO tracking control effects in dry weather.

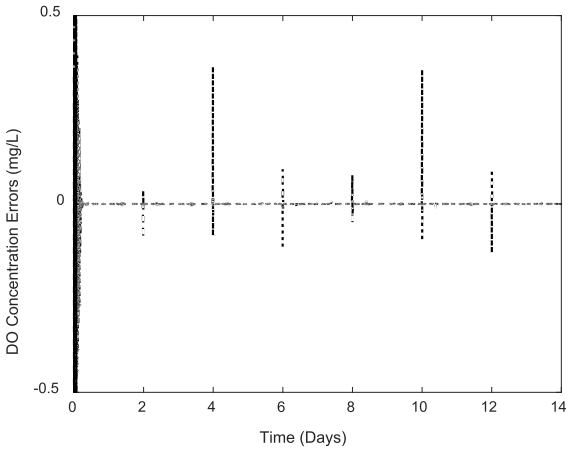

FIGURE 17. DO tracking control errors in dry weather.

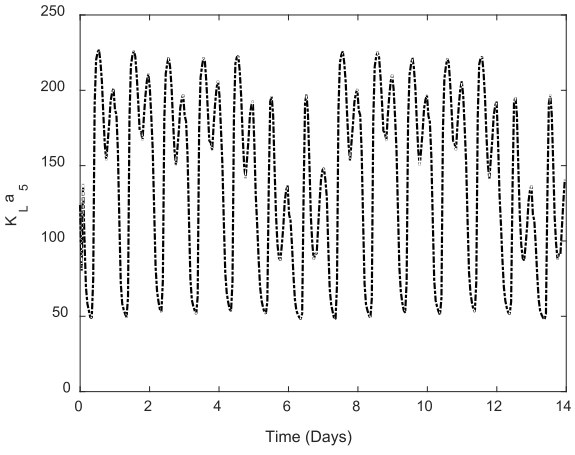

FIGURE 18. Manipulated variable $K_L a_5$ in dry weather.

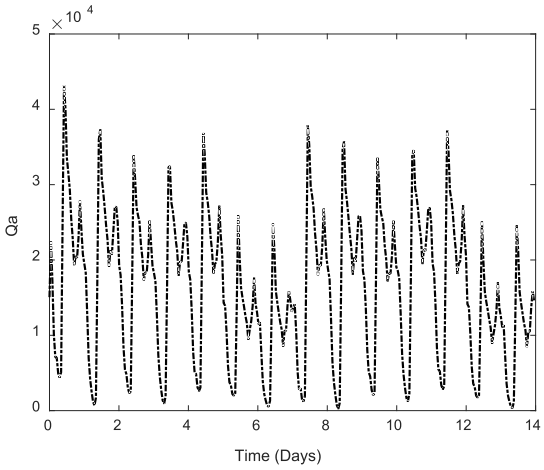

FIGURE 19. Manipulated variable *Qa* in dry weather.

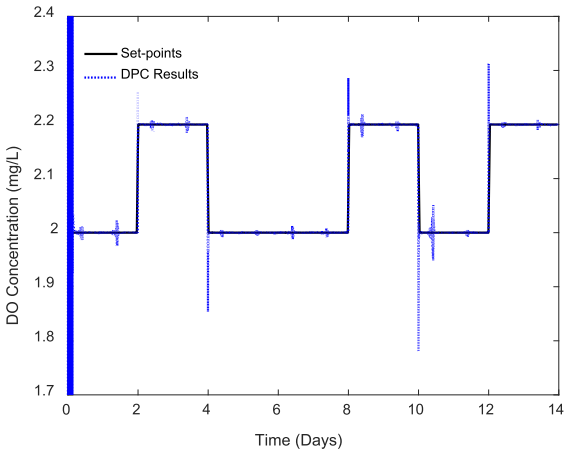

FIGURE 20. DO tracking control effects in rain weather.

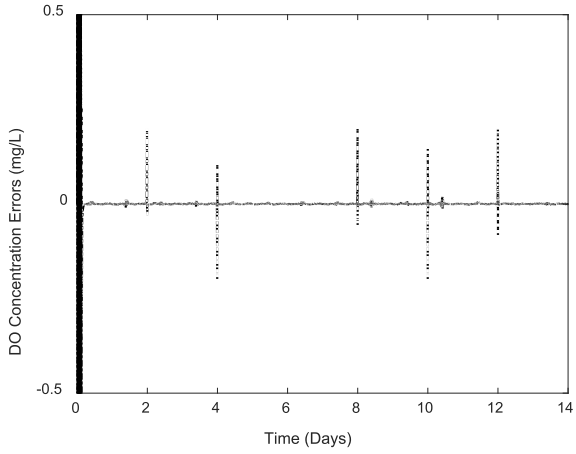

FIGURE 21. DO tracking control errors in rain weather.

reflected in Fig. 20. In Fig. 21, the differences between real outputs and set-points are displayed, and they are in the range of ± 0.02 mg/L except for the catastrophe points. Figs. 22-23 show the variation of the two manipulated variables $K_L a_5$ and Q_a, which are kept in the required ranges.

Figs. 24-27 present the tracking control results in storm weather. DO concentration tracking control results are displayed in Fig. 24 and tracking control errors are described in Fig. 25. Although the influent flow rate and influent NH_0 change obviously, the controller can adapt to the

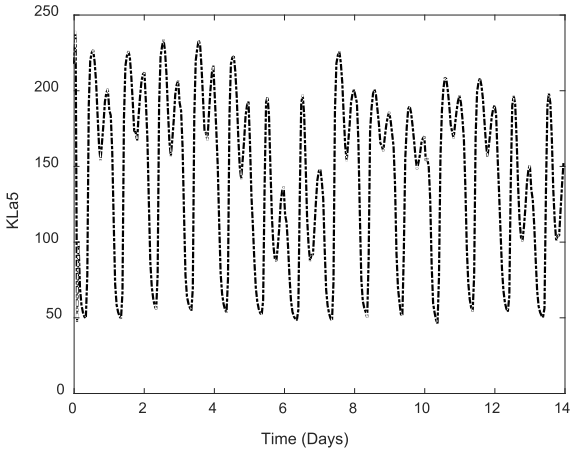

FIGURE 22. Manipulated variable $K_L a_5$ in rain weather.

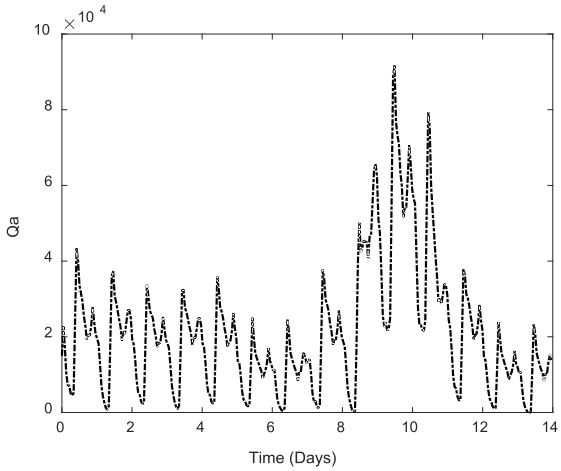

FIGURE 23. Manipulated variable Q_a in rain weather.

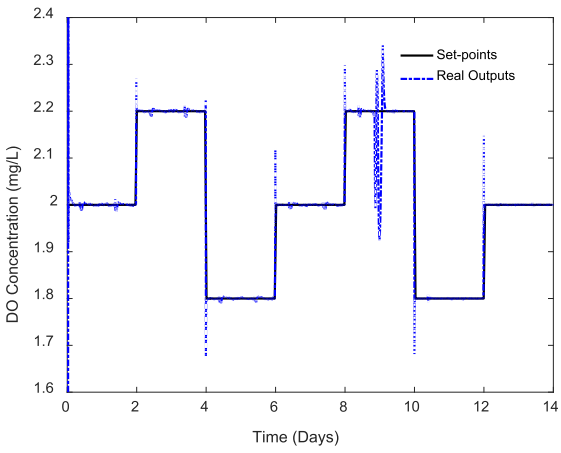

FIGURE 24. DO tracking control effects in storm weather.

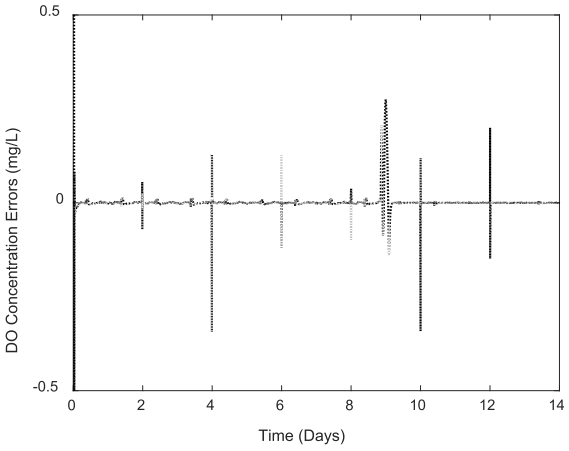

FIGURE 25. DO tracking control errors in storm weather.

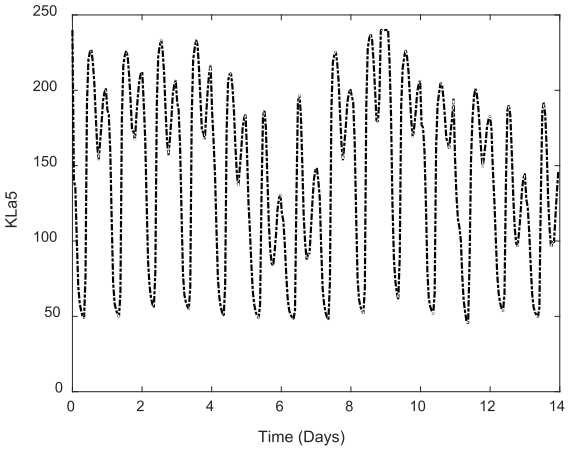

FIGURE 26. Manipulated variable $K_L a_5$ in storm weather.

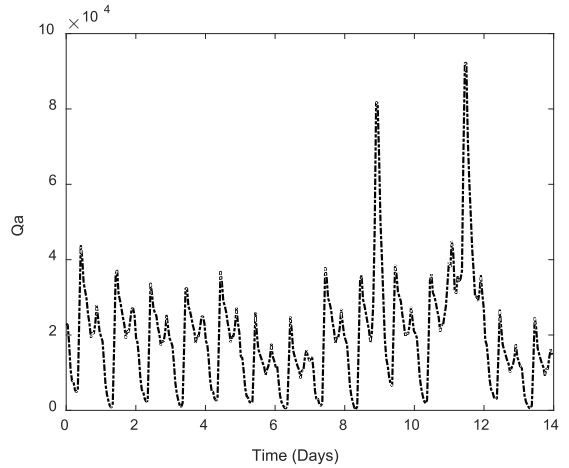

FIGURE 27. Manipulated variable Q_a in storm weather.

disturbances rapidly to guarantee the control performance. From Figs. 26-27, it can be observed that both $K_L a_5$ and Q_a can be updated smoothly to trace the set-points of DO concentration.

To evaluate the control performance, the proposed DPC strategy is also compared with other controllers that are designed for the treatment process: PI controller [3], MPC [7], ACDSNN [42], SOFC [9], SR-RBF-NMPC [27] and RBF-MPC [13]. The details of the comparisons in the three weathers are shown in Table 6.

From Table 6, it can be concluded that the proposed DPC strategy can achieve preferable control performance. The characteristics of DPC strategy can be generalized as

TABLE 6. Control performance comparison of different methods in case 2.

Weather	Controller	Rise Time (h)	Peak Time (h)	*IAE* (mg/L)	*ME* (mg/L)	*AE*(€/d)
Dry	**DPC**	**0.69**	**1.00**	**0.010**	**0.0038**	**672**
	PI [3]	0.69	1.001	0.278*	0.112	680*
	MPC [7]	0.92	1.10	0.102*	0..078*	678
	ACDSNN [42]	1.01*	--	--	0.011*	--
	SOFC [9]	1.04	1.40	0.018*	0.020*	--
	SR-RBF-NMPC [27]	--	--	0.066*	--	673*
	SORBF-MPC [13]	--	--	0.109	--	678
Rain	**DPC**	**0.72**	**1.04**	**0.013**	**0.0085**	**673**
	PI [3]	0.74	1.10	0.256*	0.130	698*
	MPC [7]	1.10	1.18	0.150*	0.094	692*
	ACDSNN [42]	1.01*	--	--	0.013*	--
	SOFC [9]	1.34	1.52		0.035	--
	SR-RBF-NMPC [27]	--	--	0.063*	--	670*
	SORBF-MPC [13]	--	--	0.119	--	689
Storm	**DPC**	**0.72**	**1.08**	**0.0119**	**0.0054**	**675**
	PI [3]	0.74	1.11	0.290	0.125	698
	MPC [7]	1.13	1.22	0.170	0.097	684
	ACDSNN [42]	1.01*	--	--	0.017*	--
	SOFC [9]	1.34	1.65	0.025*	0.097*	--
	SR-RBF-NMPC [27]	--	--	0.072*	--	677*
	SORBF-MPC [13]	--	--	0.120	--	683

'*' denotes the result is listed in the original paper, '--' denotes none

follows. At first, the proposed DPC strategy can realize the tracking control with higher control accuracy under the three weathers in spite of the time-varying optimal set-points. *IAE* and *ME* for DPC strategy in dry weather, rain weather and storm weather are 0.010 mg/L, 0.0038 mg/L, 0.013 mg/L, 0.0085 mg/L, and 0.0119 mg/L, 0.0054 mg/L respectively, which are lower than the compared PI, MPC, ACDSNN, SOFC, SR-RBF-NMPC, SOFNN-MPC methods. Meanwhile, the system time is shorter than other compared methods, the rise time and peak time in DPC strategy are 0.69 h, 1.00 h, 0.72 h, 1.04 h and 0.72 h, 1.08 h respectively. Moreover, reduced *AE* is achieved by the proposed DPC strategy, which are 672 €/d, 673 €/d and 675 €/d under the three weathers.

C. ANALYSIS OF THE RESULTS

The results presented above demonstrate that the proposed DPC strategy can realize high-accuracy DO concentration tracking control even when the process is loaded with random disturbances. Based on the former results, the proposed DPC strategy owns several superior performances.

Firstly, due to the nonlinearity and discontinuity of the measurement process in WWTP, SOFNN model makes it possible to identify DO concentration accurately, which is presented in Table 3 and Table 5. The comparison results indicate that SOFNN model is more suitable for modeling the complex WWTP. The proposed SOFNN model can update both the model parameters and structure by gradient descent algorithm and relative importance index. Therefore, SOFNN can achieve superior modeling accuracy and better generalization capability.

Secondly, the tracking control ability has been evaluated by two cases, with fixed optimal set-points and time-varying optimal set-points. From the two cases, it is evident that the proposed DPC strategy achieves satisfied control performance. The details of the control results are shown in Figs. 4-27. Minimal tracking control errors have been achieved both with fixed and time-varying optimal set-points of DO concentration. Moreover, according to the results, it is clearly observed that the average *IAE* or *ME* can be controlled well and thereby save energy of the process. These superior performance indexes depend on the model prediction accuracy and updated rules of the control sequences. Moreover, better robustness of DPC strategy has been revealed from Figs. 4, 8, 12, 16, 20 and 24, for the controller can adapt to the external disturbances rapidly to guarantee the control performance.

Thirdly, the proposed DPC strategy formed by SOFNN identifier, barrier function method and adaptive second-order L-M algorithm, has revealed its advantages for controlling DO concentration in WWTP. Moreover, the stability analysis of the control system has been proved by monotone and bounded property. This successful application of the proposed DPC strategy in constrained WWTP has developed a novel method for controlling the constrained nonlinear industrial process.

V. CONCLUSION

In this paper, a DPC scheme, based on SOFNN identifier, barrier function method and adaptive second-order L-M algorithm, is proposed to control DO concentration in WWTP.

Experimental simulations and results analysis are provided to demonstrate its prediction and on-line control performance for three different weathers under fixed and time-varying optimal set-points. It is pointed out that SOFNN model works well in WWTP. To reduce the computation complexity, barrier function method is applied to redesign the constrained cost function into a nonlinear programming problem. Adaptive second-order L-M algorithm, a fast and robust nonlinear optimization algorithm is introduced to update the control sequences. Stability of the proposed DPC strategy is proven checking the monotonicity of the cost function. Experimental results indicate that the proposed DPC strategy is competitive in terms of modelling and control performance when compared with other methods.

For a real WWTP is always running with some constraints, such as the air blow, this study provides an effective methodology for solving the constrained industrial problem. Moreover, the proposed DPC strategy can also achieve reduced complexity and satisfied control accuracy when controlling the complex industrial process. In the future, to balance the accuracy and economy, the economic model predictive control strategy will be researched, moreover, considering the multi-variable influence in WWTP, multi-objective time-varying optimal control based on DPC will be researched.

REFERENCES

[1] I. Santín, C. Pedret, R. Vilanova, and M. Meneses, "Advanced decision control system for effluent violations removal in wastewater treatment plants," *Control Eng. Pract.*, vol. 49, pp. 60–75, Apr. 2016.

[2] D.-W. Gao and Z.-D. Wen, "Phthalate esters in the environment: A critical review of their occurrence, biodegradation, and removal during wastewater treatment processes," *Sci. Total Environ.*, vol. 541, pp. 986–1001, Jan. 2016.

[3] K. Solon *et al.*, "Plant-wide modelling of phosphorus transformations in wastewater treatment systems: Impacts of control and operational strategies," *Water Res.*, vol. 113, pp. 97–110, Apr. 2017.

[4] T. Kobayashi, T. Sugai, T. Handa, Y. Minamitani, and T. Nose, "The effect of spraying of water droplets and location of water droplets on the water treatment by pulsed discharge in air," *IEEE Trans. Plasma Sci.*, vol. 38, no. 10, pp. 2675–2680, Oct. 2010.

[5] Z.-H. Pang, G.-P. Liu, D. Zhou, and D. Sun, "Data-based predictive control for networked nonlinear systems with network-induced delay and packet dropout," *IEEE Trans. Ind. Electron.*, vol. 63, no. 2, pp. 1249–1257, Feb. 2016.

[6] Z. Hou and S. Jin, "A novel data-driven control approach for a class of discrete-time nonlinear systems," *IEEE Trans. Control Syst. Technol.*, vol. 19, no. 6, pp. 1549–1558, Nov. 2011.

[7] M. Metzger and G. Polakow, "A survey on applications of agent technology in industrial process control," *IEEE Trans. Ind. Informat.*, vol. 7, no. 4, pp. 570–581, Nov. 2011.

[8] F. Wang *et al.*, "Finite control set model predictive torque control of induction machine with a robust adaptive observer," *IEEE Trans. Ind. Electron.*, vol. 64, no. 4, pp. 2631–2641, Apr. 2017.

[9] J. Qiao, W. Zhang, and H. Han, "Self-organizing fuzzy control for dissolved oxygen concentration using fuzzy neural network," *J. Intel. Fuzzy Syst.*, vol. 30, no. 6, pp. 3411–3422, Apr. 2016.

[10] S. Vazquez, J. Rodriguez, M. Rivera, L. G. Franquelo, and M. Norambuena, "Model predictive control for power converters and drives: Advances and trends," *IEEE Trans. Ind. Electron.*, vol. 64, no. 2, pp. 935–947, Feb. 2017.

[11] J. Qiu, T. Wang, S. Yin, and H. Gao, "Data-based optimal control for networked double-layer industrial processes," *IEEE Trans. Ind. Electron.*, vol. 64, no. 5, pp. 4179–4186, May 2017.

[12] H. H. Abdeltawab and Y. A.-R. I. Mohamed, "Market-oriented energy management of a hybrid wind-battery energy storage system via model predictive control with constraint optimizer," *IEEE Trans. Ind. Electron.*, vol. 62, no. 11, pp. 6658–6670, Nov. 2015.

[13] H.-G. Han, J.-F. Qiao, and Q.-L. Chen, "Model predictive control of dissolved oxygen concentration based on a self-organizing RBF neural network," *Control Eng. Pract.*, vol. 20, no. 4, pp. 465–476, Apr. 2012.

[14] T. Wang, H. Gao, and J. Qiu, "A combined adaptive neural network and nonlinear model predictive control for multirate networked industrial process control," *IEEE Trans. Neural Netw. Learn. Syst.*, vol. 27, no. 2, pp. 416–425, Feb. 2016.

[15] A. Stare, N. Hvala, and D. Vrečko, "Modeling, identification, and validation of models for predictive ammonia control in a wastewater treatment plant—A case study," *ISA Trans.*, vol. 45, no. 2, pp. 159–174, Apr. 2006.

[16] D. Vrečko, N. Hvala, and M. Stražar, "The application of model predictive control of ammonia nitrogen in an activated sludge process," *Water Sci. Technol.*, vol. 64, no. 5, pp. 1115–1121, Sep. 2011.

[17] M. Krueger, H. Luo, S. X. Ding, S. Dominic, and S. Yin, "Data-driven approach of KPI monitoring and prediction with application to wastewater treatment process," *IFAC-PapersOnLine*, vol. 48, no. 21, pp. 627–632, Sep. 2015.

[18] W. Shao and X. Tian, "Adaptive soft sensor for quality prediction of chemical processes based on selective ensemble of local partial least squares models," *Chem. Eng. Res. Des.*, vol. 95, pp. 113–132, Mar. 2015.

[19] G. M. Zeng, X. S. Qin, L. He, G. H. Huang, H. L. Liu, and Y. P. Lin, "A neural network predictive control system for paper mill wastewater treatment," *Eng. Appl. Artif. Intell.*, vol. 16, no. 2, pp. 121–129, Mar. 2003.

[20] P. Tatjewski and M. Ławryńczuk, "Soft computing in model-based predictive control," *Int. J. Appl. Math. Comput. Sci.*, vol. 16, no. 1, pp. 7–26, Jan. 2006.

[21] J. Mendes, R. Araújo, and F. Souza, "Adaptive fuzzy identification and predictive control for industrial processes," *Expert Syst. Appl.*, vol. 40, no. 17, pp. 6964–6975, Dec. 2013.

[22] T. Yang, W. Qiu, Y. Ma, M. Chadli, and L. Zhang, "Fuzzy model-based predictive control of dissolved oxygen in activated sludge processes," *Neurocomputing*, vol. 136, pp. 88–95, Jul. 2014.

[23] Q. Lu, P. Shi, H.-K. Lam, and Y. Zhao, "Interval type-2 fuzzy model predictive control of nonlinear networked control systems," *IEEE Trans. Fuzzy Syst.*, vol. 23, no. 6, pp. 2317–2328, Dec. 2015.

[24] C.-H. Lu, "Wavelet fuzzy neural networks for identification and predictive control of dynamic systems," *IEEE Trans. Ind. Electron.*, vol. 58, no. 7, pp. 3046–3058, Jul. 2011.

[25] L. Cheng, W. Liu, Z.-G. Hou, J. Yu, and M. Tan, "Neural-network-based nonlinear model predictive control for piezoelectric actuators," *IEEE Trans. Ind. Electron.*, vol. 62, no. 12, pp. 7717–7727, Dec. 2015.

[26] Z. Yan and J. Wang, "Robust model predictive control of nonlinear systems with unmodeled dynamics and bounded uncertainties based on neural networks," *IEEE Trans. Neural Netw. Learn. Syst.*, vol. 25, no. 3, pp. 457–469, Mar. 2014.

[27] H.-G. Han, L. Zhang, Y. Hou, and J.-F. Qiao, "Nonlinear model predictive control based on a self-organizing recurrent neural network," *IEEE Trans. Neural Netw. Learn. Syst.*, vol. 27, no. 2, pp. 402–415, Feb. 2016.

[28] M. N. Zeilinger, C. N. Jones, and M. Morari, "Real-time suboptimal model predictive control using a combination of explicit MPC and online optimization," *IEEE Trans. Autom. Control*, vol. 56, no. 7, pp. 1524–1534, Jul. 2011.

[29] M. A. Müller and F. Allgöwer, "Improving performance in model predictive control: Switching cost functionals under average dwell-time," *Automatica*, vol. 48, no. 2, pp. 402–409, Feb. 2012.

[30] R. Amrit, J. B. Rawlings, and L. T. Biegler, "Optimizing process economics online using model predictive control," *Comput. Chem. Eng.*, vol. 58, pp. 334–343, Nov. 2013.

[31] M. Mulas *et al.*, "Predictive control of an activated sludge process: An application to the Viikinmäki wastewater treatment plant," *J. Process Control*, vol. 35, pp. 89–100, Nov. 2015.

[32] J. H. Lee, "Model predictive control: Review of the three decades of development," *Int. J. Control, Autom. Syst.*, vol. 9, no. 3, pp. 415–424, Jun. 2011.

[33] Y. Pan and J. Wang, "Model predictive control of unknown nonlinear dynamical systems based on recurrent neural networks," *IEEE Trans. Ind. Electron.*, vol. 59, no. 8, pp. 3089–3101, Aug. 2012.

[34] P. D. Christofides, R. Scattolini, D. M. de la Peña, and J. Liu, "Distributed model predictive control: A tutorial review and future research directions," *Comput. Chem. Eng.*, vol. 51, pp. 21–41, Apr. 2013.

[35] S. Tonidandel and J. M. LeBreton, "Relative importance analysis: A useful supplement to regression analysis," *J. Bus. Psychol.*, vol. 26, no. 1, pp. 1–9, Mar. 2011.
[36] S. Tonidandel, J. M. LeBreton, and J. W. Johnson, "Determining the statistical significance of relative weights," *Psychol. Methods*, vol. 14, no. 4, pp. 387–399, Dec. 2009.
[37] H. Han and J. Qiao, "A self-organizing fuzzy neural network based on a growing-and-pruning algorithm," *IEEE Trans. Fuzzy Syst.*, vol. 18, no. 6, pp. 1129–1143, Dec. 2010.
[38] H.-G. Han, X.-L. Wu, and J.-F. Qiao, "Real-time model predictive control using a self-organizing neural network," *IEEE Trans. Neural Netw. Learn. Syst.*, vol. 24, no. 9, pp. 1425–1436, Sep. 2013.
[39] H. Han, L. Zhang, X. Wu, and J. Qiao, "An efficient second-order algorithm for self-organizing fuzzy neural networks," *IEEE Trans. Cybern.*, to be published.
[40] A. G. Wills and W. P. Heath, "Barrier function based model predictive control," *Automatica*, vol. 40, no. 8, pp. 1415–1422, Aug. 2004.
[41] V. Chandramouli, G. Brion, T. R. Neelakantan, and S. Lingireddy, "Backfilling missing microbial concentrations in a riverine database using artificial neural networks," *Water Res.*, vol. 41, no. 1, pp. 217–227, Jan. 2007.
[42] H.-G. Han and J.-F. Qiao, "Adaptive dissolved oxygen control based on dynamic structure neural network," *Appl. Soft Comput.*, vol. 11, no. 4, pp. 3812–3820, Jun. 2011.
[43] M. Bortman and M. Aladjem, "A growing and pruning method for radial basis function networks," *IEEE Trans. Neural Netw.*, vol. 20, no. 6, pp. 1039–1045, Jun. 2009.
[44] S. Wu and M. J. Er, "Dynamic fuzzy neural networks-a novel approach to function approximation," *IEEE Trans. Syst., Man, Cybern. B, Cybern.*, vol. 30, no. 2, pp. 358–364, Apr. 2000.

HONG-GUI HAN (SM'15) received the B.S. degree in automatic from the Civil Aviation University of China, Tianjin, China, in 2005, and the M.E. and Ph.D. degrees from the Beijing University of Technology, Beijing, China, in 2007 and 2011, respectively.

He has been with the Beijing University of Technology since 2011, where he is currently a Professor. His current research interests include neural networks, fuzzy systems, intelligent systems, modeling and control in process systems, and civil and environmental engineering.

Prof. Han is a member of the IEEE Computational Intelligence Society. He is currently a Reviewer of the IEEE TRANSACTIONS ON FUZZY SYSTEMS, the IEEE TRANSACTIONS ON NEURAL NETWORKS AND LEARNING SYSTEMS, the IEEE TRANSACTIONS ON CYBERNETICS, the IEEE TRANSACTIONS ON CONTROL SYSTEMS TECHNOLOGY, the *Control Engineering Practice*, and the *Journal of Process Control*.

LU ZHANG received the B.E. degree in automatic control from Heze University, Heze, China, in 2014. She is currently pursuing the Ph.D. degree with the College of Electronic and Control Engineering, Beijing University of Technology, Beijing, China.

Her current research interests include neural networks, intelligent systems, modeling and control in process systems.

JUN-FEI QIAO (M'11) received the B.E. and M.E. degrees in control engineering from Liaoning Technical University, Fuxin, China, in 1992 and 1995, respectively, and the Ph.D. degree from Northeast University, Shenyang, China, in 1998.

From 1998 to 2000, he was a Post-Doctoral Fellow with the School of Automatics, Tianjin University, Tianjin, China. He joined the Beijing University of Technology, where he is currently a Professor. He is the Director of the Intelligence Systems Laboratory. His research interests include neural networks, intelligent systems, self-adaptive/learning systems, and process control systems.

Prof. Qiao is a member of the IEEE Computational Intelligence Society. He is currently a reviewer for over 20 international journals, such as the IEEE TRANSACTIONS ON FUZZY SYSTEMS, the IEEE TRANSACTIONS ON NEURAL NETWORKS AND LEARNING SYSTEMS.